Korean J. Chem. Eng., **30**(10), 1918-1928 (2013)
DOI: 10.1007/s11814-013-0113-9

Biofiltration of volatile organic compound using two packing materials: Kinetics and modelling

Viswanathan Saravanan*,†, Manivasagan Rajasimman*, and Natarajan Rajamohan**

*Department of Chemical Engineering, Annamalai University, Annamalai Nagar-608002, Tamilnadu, India
**Sohar University, Sohar, Sultanate of Oman
(*Received 6 May 2013 • accepted 26 June 2013*)

Abstract−The performance of two laboratory scale biofilters, packed with pressmud (BF1) and sugarcane bagasse (BF2), was evaluated for gas phase ethylacetate removal under various operating conditions. Biofilters were inoculated with mixed culture obtained from pharmaceutical wastewater sludge. Experiments were carried out at different flow rates (0.03, 0.06, 0.09 and 0.12 $m^3\ h^{-1}$) and inlet ethylacetate concentrations (0.2, 0.4, 0.6 and 1.2 gm^{-3}). Maximum removal efficiency (RE) of 100% and 98% was achieved at an inlet concentration of 0.2 gm^{-3} and gas flow rate of 0.03 $m^3\ h^{-1}$ in BF1 and BF2, respectively. A maximum elimination capacity (EC) of 66.6 $gm^{-3}\ h^{-1}$ and 64.1 $gm^{-3}\ h^{-1}$ was obtained in BF1 and BF2, respectively, at an inlet concentration of 0.8 gm^{-3} and a gas flow rate of 0.12 $m^3\ h^{-1}$. The kinetics of biofiltration of ethylacetate was studied by using Ottengraf and van den Oever model. The kinetic modelling gives an insight into the mechanism of biofiltration. The modified Ottengraf model, which was also tested, demonstrated good agreement between calculated and experimental data.

Key words: Ethylacetate, Biofiltration, Ottengraf and van den Oever Model, Pressmud, Sugarcane Bagasse, Gas Flow Rate

INTRODUCTION

Volatile organic compounds (VOCs) are generally toxic gases emitted from wastewater treatment plants and many industries, such as printing and coating facilities, chemical industries, electronics, and paint manufacturing. Legislation has already been introduced to reduce their emissions due to their potential threat to the environment and human health. Conventional control technologies for VOCs, including incineration, condensation, adsorption, absorption, ozonation, and membrane separation, have been commonly utilized for the elimination of VOCs from waste gases [1]. Activated carbon has undoubtedly been the most popular and widely used adsorbent in exhaust gas treatment throughout the world because of its high surface area and pore volume [2]. Biofiltration, an effective and economical method, has gained much attention in eliminating VOCs. Compared with conventional physicochemical technologies, biological treatment technologies present the advantage of complete degradation of the contaminants into less-contaminating products [3]. However, biological processes rely solely on the capability of specific microbial species to oxidize the targeted organic pollutants. Biodegradation of organic contaminants to mineral products occurs in steps, producing intermediate compounds. An overloaded biofilter may result in high effluent concentration of untreated gases [4]. For these reasons, bioreactors are sensitive to surges in VOC loadings, and therefore biological methods are not suitable for treating waste gases containing relatively high concentrations of VOCs [5].

As the polluted air stream passes through the filter bed, pollutants are transferred from the vapor phase to the biofilm developed on the organic substrate and are metabolized by the microorganisms. Bohn (1996) reported the important physical, chemical and biological characteristics to be considered while selecting a filter medium are (i) large specific surface area, (ii) low bulk density, (iii) a high void fraction, (iv) large number of different bacteria naturally present in the carrier, (v) sufficient nutrients, i.e., N, P and K, (vi) large Water Holding Capacity and (vii) a neutral or alkaline pH as well as buffer capacity [7].

Recently, there has been an increasing demand for easily available and inexpensive raw material, to be used as solid support in biofilters [8]. In addition, the possibility of using a waste as packing material for off-gases treatment is particularly attractive [9].

Sugar cane bagasse and pressmud are agricultural residues generated from industrial sugar extraction. Although utilized in the sugar factories as fuel for the boilers, large quantities are accumulated in the mills, creating environmental problems.

Ethyl acetate (EA) is the key pollutant present in the exhaust air from printing and coating facilities and paint manufacturing. The influence of the media and operating conditions on the biofiltration of EA has been reported by several researchers. Chan and Zheng (2005) [10] investigated elimination of EA in biofilters packed with poly vinyl alcohol and pig manure compost composite beads and reported a maximum elimination capacity (EC) of 0.71 $kgm^{-3}h^{-1}$. Bibeau et al. (1997) [11] reported a maximum EC of 70 g $m^{-3}h^{-1}$ for an inlet load (IL) of 100 g $m^{-3}h^{-1}$ in a peat biofilter. Tang and Hwang (1997) [12] obtained maximum EC of 58, 60, and 97 g $m^{-3}h^{-1}$ in three biofilters packed with mixtures of chaff/compost, diatomaceous earth/compost and granular activated carbon/compost, respectively. In this paper, biofiltration of EA was carried out using two agro wastes as packing material, and the kinetics of biofiltration was studied by Ottengraf model and modified Ottengraf model.

†To whom correspondence should be addressed.
E-mail: sarav304@gmail.com

MATHEMATICAL MODELING WITH OTTENGRAF-VAN DEN OEVER MODEL

Most of the studies conducted on biofiltration utilize bacterial strains, either pure or isolated from the filtering media, suspended in liquid growth media [13-20]. The drawbacks of these methods are that (1) they necessitate prior operations for the conditioning of the biomass; (2) they do not necessarily represent the real growth media (the solid bed pellets), which more likely contain consortia of interacting micro-organisms, among them the degrading species; and (3) they do not reflect the mass transfer constraints that exist in a biofilter. To date, only a few works have focused on the experimental protocols for application to solid growth media [21]. Since many different phenomena contribute to the effectiveness of the biofiltration process, the model must comprehensively foresee bioreactor performance. Ottengraf and Van den Oever (1983) [22] made the first attempt to develop a model for the biofiltration of toluene. This model simply deals with a conventional biofilter at the stationary state. In spite of its simplicity, this model has been widely used by others [23-25]. Ottengraf's model considers the different phenomena ruling biofilter performance: mass transfer and biological reaction. At low inlet concentrations, the driving force ruling the mass transfer is limited. Therefore, the amount of pollutant which passes into the liquid phase is moderate and, as pollutant comes in contact with the biomass, it is completely degraded. In these conditions, diffusion is the rate determining step. With higher gas concentrations, mass transfer is inversely promoted. The amount of pollutant transferred in the aqueous phase is greater and biomass could not be able to completely degrade this amount. In such conditions, the reaction limits the process rate. Ottengraf proposed equations to represent what occurs in the water film in these two opposite situations.

1. Mass Balance

Pollutant concentration in the gas phase can be expressed by the following expression:

$$-U_g\frac{dU_g}{dh}=NA_S \tag{1}$$

where U_g is the superficial gas velocity (mh^{-1}), h is the reactor height (m), N is the flux of substrate from the gas to the solid ($gm^{-2}h^{-1}$) and A_s is the specific surface area (m^2m^{-3}).

A mass balance in the gas/biofilm can be written as follows:

$$D\frac{d^2C}{dx^2}-k_0=0 \tag{2}$$

where D is the diffusion coefficient (m^2h^{-1}), x is the direction perpendicular to the gas-solid interface and k_0 the zero-order constant ($gm^{-3}h^{-1}$). Such equations can be solved considering the different boundary conditions in reaction limitation and diffusion limitation assumptions.

2. Zero-order Kinetics with Reaction Limitation

In this condition, introducing 'm' as the dimensionless gas-solid partition coefficient, the following boundary conditions can be used:

$$x=0,\quad C=C_g/m \tag{3}$$

$$x=\delta,\quad dC/dx=0 \tag{4}$$

and Eq. (2) has the following solution:

$$\frac{C}{C_g/m}=1+\frac{1}{2}\frac{\Phi^2}{C_i/C_o}(\sigma^2-2\sigma) \tag{5}$$

Where Thiele number $\sigma=x/\delta$ is the dimensionless length coordinate in the biolayer, and $m(=(C_g/C_l)_{equilibrium})$ is the distribution coefficient.

$$\phi=\sqrt{\frac{k_m}{D'C_{go}}} \tag{6}$$

Then, N can be written as

$$N=\frac{-D'\left(\frac{dC_l}{d\sigma}\right)_{\sigma=0}}{\delta}=k\delta \tag{7}$$

Substituting Eq. (7) into Eq. (1) using the boundary condition $C_g=C_g$, in for h=0, the solution becomes:
where H is the height of the tower. Assuming $A_sk_o\delta=K$ to be constant, it follows that

$$\frac{C_o}{C_i}=1-\frac{A_sk_o\delta H}{C_iU_g} \tag{8}$$

$$\eta=1-\frac{C_o}{C_i}=\frac{A_sk_o\delta H}{C_{g,in}U_g} \tag{9}$$

Elaborating Eq. (8), and solving as function of the elimination capacity, the following expression can be obtained [25]

$$EC=EC_{max}=A_sk_o\delta \tag{10}$$

A critical point can be determined, supposing that C=0 at the water-solid interface, or when $x=\delta$ Substituting this value into Eq. (5), the critical Thiele number can be determined:

$$\phi=\delta\sqrt{\frac{k_om}{D'C_i}}=\sqrt{2} \tag{11}$$

When $\varphi<\Phi$cr, reaction is the rate determining step of the process.

3. Zero-order Kinetics with Diffusion Limitation

The mass balance into the (air/biofilm) phase should be now solved using different boundary conditions. Defining λ as the distance from the interface gas/liquid at which C=0, boundary condition (4) can be substituted by the following:

$$x=\lambda \quad dC/dx=0 \tag{12}$$

Obtaining a new equation for the water phase:

$$\frac{C}{C_o/m}=1+\frac{1}{2}\frac{\Phi^2}{C_i/C_o}\left(\sigma^2-2\sigma\frac{\lambda}{\delta}\right) \tag{13}$$

λ can be easily determined with Eq. (13), fixing C=0 for $\sigma=\lambda/\delta$:

$$\lambda=\sqrt{2\frac{D'C_o}{km}} \tag{14}$$

With this new condition, $N=k_0\lambda$ and pollutant concentration in the gas phase can be calculated:

$$\frac{C_o}{C_i}=\left(1-\frac{A_sH}{U_g}\sqrt{\frac{k_oD}{2C_im}}\right) \tag{15}$$

EC is now a function of the mass loading rate and the correlation is represented by the following expression:

Table 1. Physical and chemical characteristics of packing material before biofiltration

S. no	Parameters	Sugarcane bagasse	Pressmud
Physical properties			
1.	Particle diameter (cm)	1-2	2-4
2.	pH	6.24	6.2
3.	Moisture content (at field capacity) (%)	65	80
4.	Specific gravity	1.45	1.29
5.	Wet filled weight (g)	180	210
6.	Dry filled weight	121	150
7.	BET surface area ($m^2 \cdot g$)	4.146	5.3
8.	Total pore volume of pores ($cm^3 \cdot g$)	0.0041	0.0067
9.	Average pore diameter (A^o)	39.429	32.13
10	Maximum pore volume ($cm^3 \cdot g$)	0.009	0.013
11	Median pore diameter (A^o)	4887.11	5208
Chemical properties (%)			
12	C	43.22	47
13	H	6.097	2.8
14	N	0.006	0.009
15	S	0.81	0.99
16	O*	43.52	44
17	Ash	5.7	5.49

O* = 100 − (C+H+N+S) − Ash

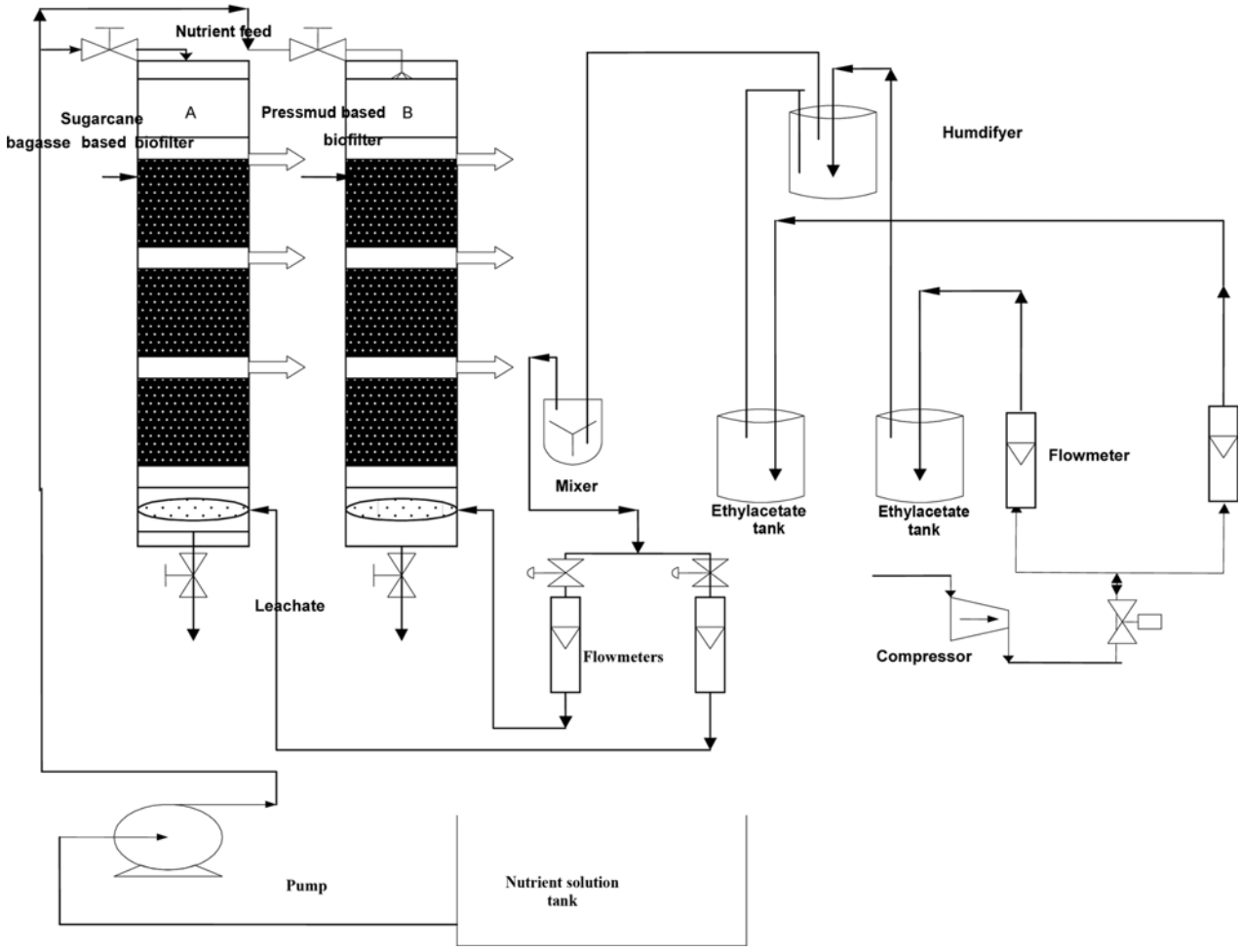

Fig. 1. Schematic diagram for biofilter for the removal of ethylacetate using pressmud and sugarcane bagasse as packing material.

$$EC = L\left(1-\left(1-A_s\sqrt{\frac{k_oD}{2m}}\sqrt{\frac{V}{QL}}\right)^2\right) \quad (16)$$

MATERIALS AND METHODS

1. Biofiltration Equipment

An upflow mode biofilter was employed in this study that consists of two columns: (i) pressmud based biofilter (BF1) and (ii) sugarcane bagasse based biofilter (BF2). The characteristics of packing materials are given in Table 1. The biofilter was equipped with additional auxiliary units like flow meters, manometers, nutrient recirculation peristaltic pump, compressor and nutrient storage vessel.

2. Packed Columns

The two columns used in this study were made of acrylic material. A detailed sketch of the packed bed biofilter isshown in Fig. 1. Both columns were 100 cm high with an internal diameter of 5 cm. A fully packed column had three sections: a 12.5 cm high empty space at the bottom (gas distribution section and leachate collection), followed by a 75 cm height of packing medium and a 12.5 cm height of empty space at the top (nutrient distribution system and outlet collection). The filter bed had three layers and each layer had a height of 25 cm. The packing material was mixed with berl saddles and packed into the column. The berl saddles were used to prevent bed compaction for organic packing media. The volume of packing media was 1.47 L. Each column had three ports for measuring outlet concentration of ethylacetate.

3. Operating Conditions and Experimental Control

The activated sludge obtained from a pharmaceutical industry plant was used as inoculum. The biofilter was operated continuously for more than 160 days. A nutrient solution containing 10.0 g L^{-1} of $NaNO_3$, 0.7 g L^{-1} of Na_2HPO_4, 0.5 g L^{-1} of KH_2PO_4 and other trace elements was added into the filter bed from the top of the biofilter periodically to supply the nutrient for the growth of microorganisms.

Table 2. Operating conditions of the biofilers for the biofiltraion of ethylacetate

Phase	Operating days	Average inlet concentration ($g \cdot m^{-3}$)	Flow rate (m^3h^{-1})
I	0-10	0.2	0.03
	11-20		0.06
	21-30		0.09
	31-40		0.12
II	41-50	0.4	0.03
	51-60		0.06
	61-70		0.09
	71-80		0.12
III	81-90	0.8	0.03
	91-100		0.06
	101-110		0.09
	111-120		0.12
VI	121-130	1.2	0.03
	131-140		0.06
	141-150		0.09
	151-160		0.12

The operation of biofilter was divided into four stages (Table 2). In each stage, the biofiltration of ethylacetate was performed at different inlet concentrations (0.2-1.2 gm^{-3}) and gas flow rates (0.03 m^3h^{-1} to 0.12 m^3h^{-1}).

4. Analytical Methods

Ethylacetate concentrations were analyzed by a gas chromatograph (Nucon5655, Amil Limited, India) with an FID detector. The carrier gas selected was nitrogen and the temperature of column oven, injector and detector was 150, 250 and 250 °C, respectively. The CO_2 concentrations were analyzed by the same gas chromatograph with a TCD detector and a stainless steel column (3 mm× 2 m). The carrier gas was nitrogen and the temperature of the column oven, the injector and the detector was 130, 150 and 100 °C, respectively. The results obtained were given in terms of removal efficiency. The inlet load ($gm^{-3}h^{-1}$), elimination capacity ($gm^{-3}h^{-1}$) and removal efficiency RE (%) were calculated by using the following equations [2]:

$$RE = \frac{C_{gi}-C_{go}}{C_{ig}} \times 100 \quad (17)$$

$$IL = \frac{QC_{gi}}{V} \quad (18)$$

$$EC = \frac{Q(C_{gi}-C_{go})}{V} \quad (19)$$

$$EBRT = \frac{V}{Q} \quad (20)$$

where RE is the removal efficiency (%), C_{gi} is the inlet toluene concentration ($g \cdot m^{-3}$) ,C_{go} is the outlet toluene concentration ($g \cdot m^{-3}$), V is the volume of the reactor (m^3) and Q is the volumetric flow rate (m^3h^{-1}).

RESULTS AND DISCUSSION

1. Biofiltration of EA Using Pressmud and Sugarcane Bagasse as Packing Material

The biofiltration of gas stream containing EA was carried out for 160 days at various operating conditions in an up flow mode pressmud (BF1) and sugarcane bagasse (BF2) based biofilters. Each biofilter was operated in four stages, and each stage was divided into four phases.

In the present work, the combined effect of the ethylacetate inlet concentration and the gas flow rate on the biofilter performance was investigated by two packing materials, BF1and BF2. Figs. 2 and 3 show the RE and outlet concentration of EA for various inlet EA concentration (0.2-1.2 $g \cdot m^{-3}$) and gas flow rates (0.03-0.12 m^3h^{-1}) in BF1 and BF2, respectively. Figs. 4 and 5 present the elimination capacity as a function of the inlet load for each gas flow rate in BF1 and BF2, respectively.

At a gas flow rate of 0.03 $m^3 h^{-1}$ and inlet concentration of 0.2 gm^{-3}, the removal of ethylacetate was 100% in BF1 and 98% n BF2. The RE decreased to 80% and 75% in BF1 and BF2 when the inlet concentration increased from 0.4 gm^{-3} to 1.2 gm^{-3}. The results are shown in Figs. 2 and 3. At this gas flow rate, for an IL of 16 $gm^{-3}h^{-1}$, (corresponding to inlet concentrations of 0.4 gm^{-3}), EC was observed to increase with IL. But at higher IL (100 $gm^{-3}h^{-1}$), the EC decreased.

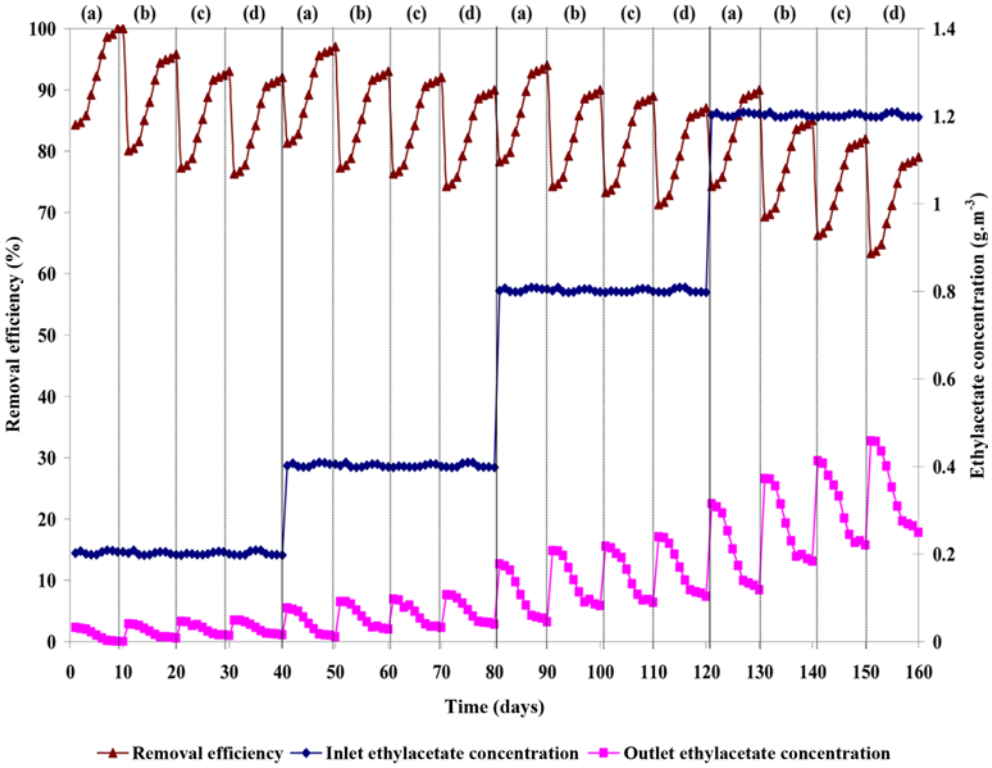

Fig. 2. Experimental results of continuous ethylacetate removal using pressmud as packing material - gas flow rate - (a) 0.03 m^3h^{-1} (b) 0.06 m^3h^{-1} (c) 0.09 m^3h^{-1} and (d) 0.12 m^3h^{-1}.

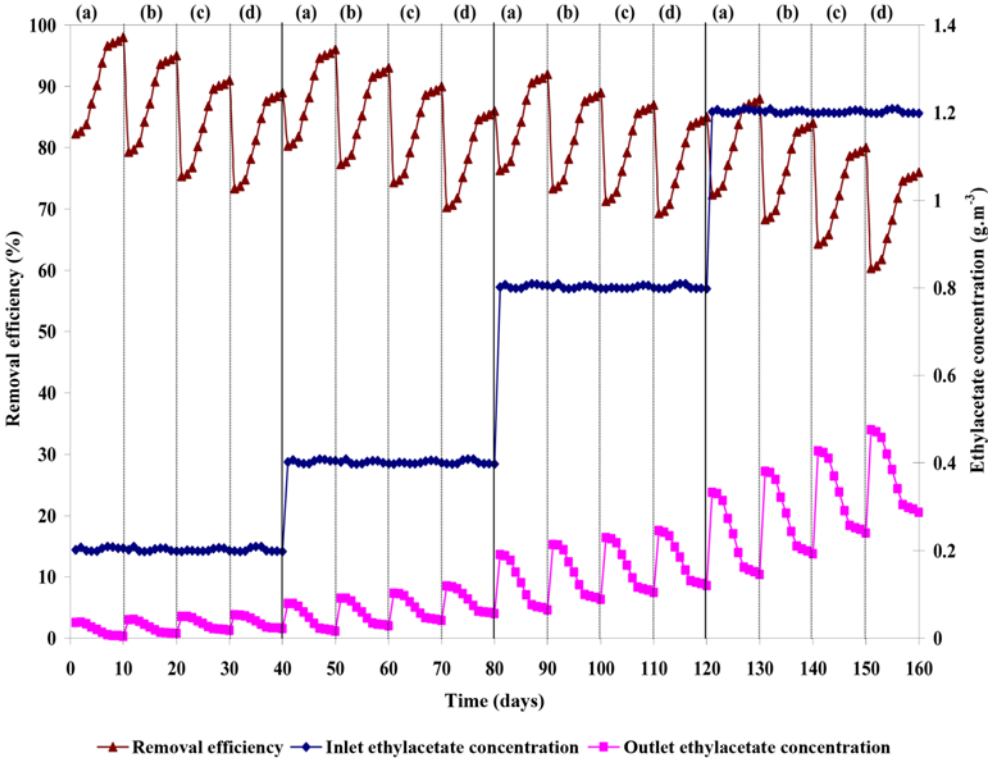

Fig. 3. Experimental results of continuous ethylacetate removal using sugarcane bagasse - packing material. Gas flow rate - (a) 0.03 m^3h^{-1} (b) 0.06 m^3h^{-1} and (c) 0.09 m^3h^{-1} (d) 0.12 m^3h^{-1}.

At a gas flow rate of 0.06 m^3 h^{-1}, with ethylacetate concentrations varying from 0.2 gm^{-3} to 1.2 gm^{-3}, the RE decreased from 94% to 82% in BF1 and 92% to 80% in BF2. This is clearly depicted in Figs. 2 and 3. At this gas flow rate, the EC of ethylacetate increased

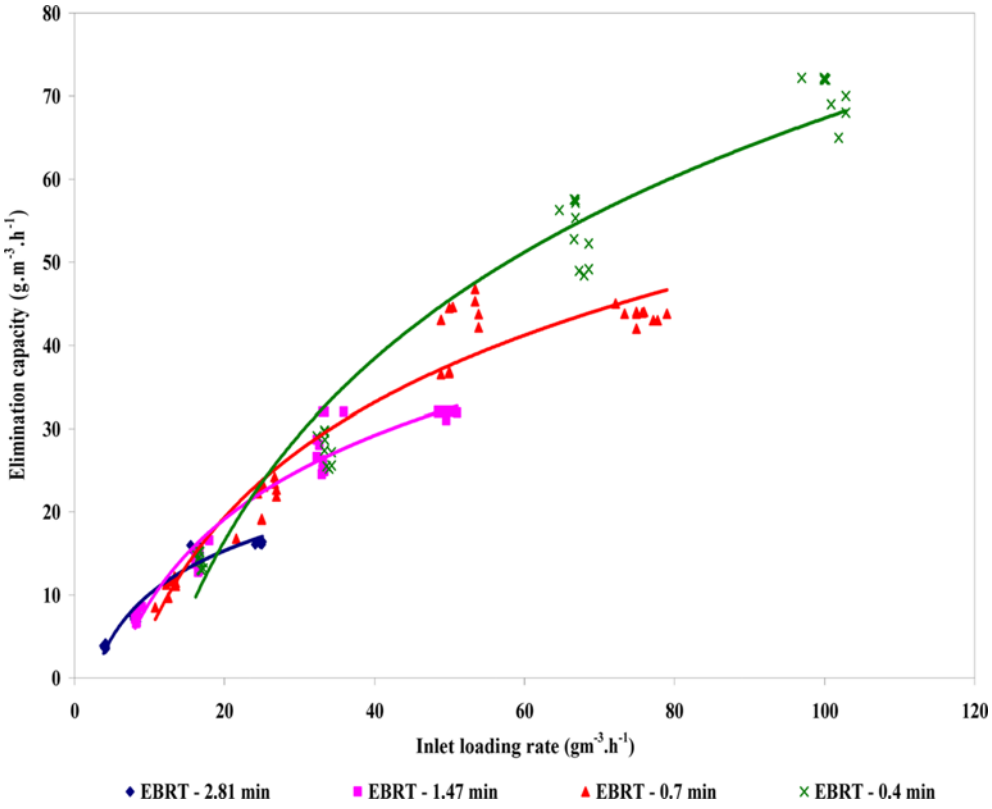

Fig. 4. Elimination capacity of ethylacetate at various ethylacetate inlet loads and different gas flow rates for pressmud based biofilter.

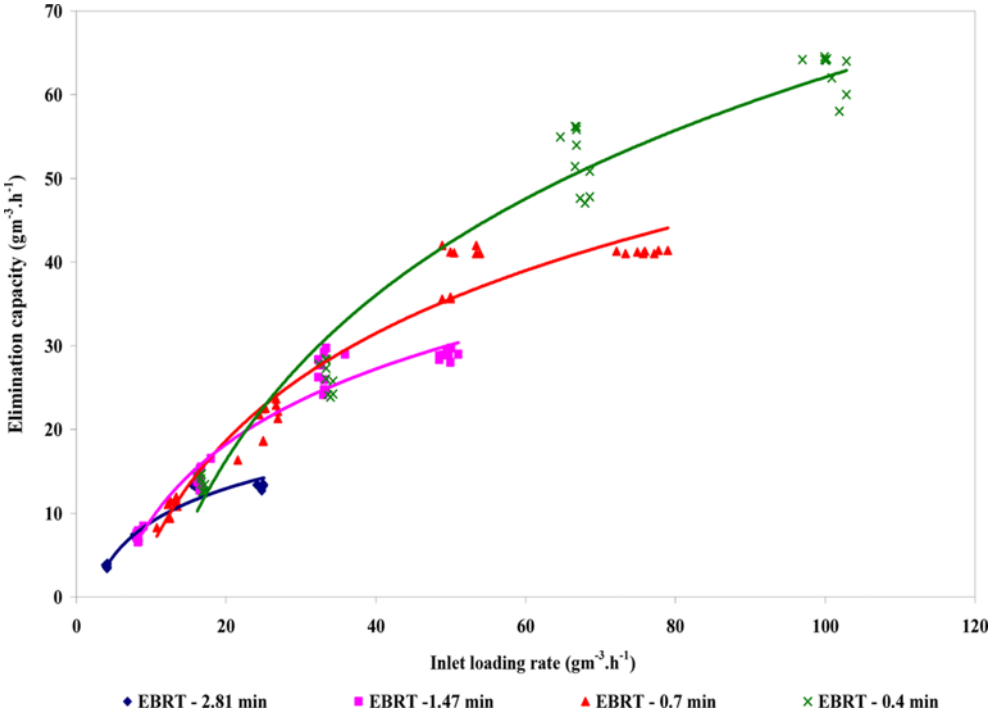

Fig. 5. Elimination capacity of ethylacetate at various ethylacetate inlet loads and different gas flow rates for sugarcane bagasse based biofilter.

up to an IL of 16 gm^{-3} h^{-1} and 30 gm^{-3} h^{-1} in BF1 and BF2, respectively, and then decreased.

It was inferred from Fig. 2 that at a gas flow rate of 0.09 m^3 h^{-1}, the removal of ethylacetate decreased for inlet concentrations ranging from 0.2 gm^{-3} to 1.2 gm^{-3} in both the biofilters. For loads smaller than 60 gm^{-3} h^{-1}, EC increased with IL to a maximum of 41 gm^{-3}

Table 3. Model parameters and kinetic constants at various operating conditions for both packing materials for the biofiltration of EA

Packing material	C_i (gm^{-3})	GF (m^3h^{-1})	IL ($gm^{-3}h^{-1}$)	k_1 ($gm^{-3}h^{-1}$)	k_d ($gm^{-3}h^{-1}$)	k_0 $gm^{-3}h^{-1}$	$C_{Critical}$ (gm^{-3})	$IL_{Critical}$ ($gm^{-3}h^{-1}$)	δ (μm)
Pressmud	0.2-1.2	0.03	4.16-25.02	0.741	0.252	16.45	0.931	21	267
		0.06	12.48-50.04	0.735	0.312	30.25	0.931	38	289
		0.09	18.72-75.06	0.727	0.202	66.61	0.898	55	346
		0.12	24.96-100.08	0.680	0.235	72.2	0.92	76	401
Sugarcane bagasse	0.2-1.2	0.03	4.16-25.02	0.884	0.322	15.22	1.078	22	260
		0.06	12.48-50.04	0.807	0.199	29.12	0.808	33	275
		0.09	18.72-75.06	0.761	0.171	64.1	0.849	52	321
		0.12	24.96-100.08	0.513	0.047	66.6	0.906	74	361

h^{-1} and 35 gm^{-3} h^{-1} in BF1 and BF2, respectively, and decreased for higher ethylacetate loads. Similar trend was observed for the gas flow rate of 0.12 m^3 h^{-1}. A maximum elimination capacity of 66.6 gm^{-3} h^{-1}, in BF1 and 64.1 gm^{-3} h^{-1}, in BF2 was achieved at inlet concentration of 0.8 gm^{-3} and a gas flow rate of 0.12 m^3 h^{-1}. In both the biofilters, nearly 100% removal was achieved at a gas flow rate of 0.03 m^3 h^{-1}. When the gas flow rate was increased, the EC at constant IL and RE at constant ethyl acetate inlet concentration were found to decrease. This is because of decreased contact time between the pollutant and the microbial population at higher gas flow rate. EC was found to increase with IL up to a certain value 55 gm^{-3} h^{-1} and decreased with further increase in inlet concentration. The increase in EC with the increase of the ethylacetate inlet concentration is due to enhanced transfer rate of ethylacetate from the gas phase to the biofilm, so that more microorganisms participated in the biodegradation activity. This behavior can be described as a diffusion limitation regime. As IL increased above the upper limit of the diffusion limitation regime, EC decreased. Other studies reported similar behavior for EC of 225 gm^{-3} h^{-1} [26] and 120 gm^{-3} h^{-1} [27].

2. Application of the Theoretical Model

According to Eq. (11), the outlet concentration of EA, in the situation of diffusion limitation, can be described by the following equation:

$$\sqrt{C_i} = \sqrt{C_o} - k_1 \frac{V}{Q} \tag{20}$$

Hence, in the case of diffusion limitation, the validity of the theoretical model can be checked by plotting $\sqrt{C_i}$ versus the range of inlet concentrations ($\sqrt{C_o}$) for which the EC is less than the k_o. According to Eq. (20), the theoretical diffusion model can be judged to be appropriate if the experimental points are on a line with a slope equal to 0.6. By knowing the gas flow rate and the filter bed volume, the constant of the line equation enables one to estimate the parameter k_1. The reaction limitation behavior is attained at a level of pollutant load that corresponds, at a given gas flow rate, to the critical inlet concentration at which the biofilter behavior is in transition between the diffusion and the reaction limitation. Therefore, the critical concentration of EA can be estimated from the following relationship:

$$EC = \frac{Q}{V} C_{o,Crit} L\left(1 - \left(1 - k_1 \frac{V}{Q} \frac{1}{\sqrt{C_{o,crit}}}\right)^2\right) = k_o \tag{21}$$

Hence,

$$C_{o,Crit} = \frac{1}{4}\left(\frac{k_o}{k_1} + \frac{k_1 V}{Q}\right)^2 \tag{22}$$

The model is tested for the biofiltration of EA using pressmud and sugarcane bagasse based biofilter. For each packing material, the plot has a portion displaying increasing elimination capacity with pollutant load, which can be identified by the diffusion limitation behavior, and a portion displaying constant elimination capacity, which is attributed to the reaction limitation behavior. Thus, diffusion limitation is valid for low concentrations, and the theoretical reaction limitation model seems to be valid for high concentrations of EA in both BF1 and BF2. The values of model parameters, kinetic constants and maximum EC for at different operating conditions are tabulated in Table 3.

The biofilm thickness was also calculated for different phases using Eq. (11) by taking the values of effective diffusivity of biofilm (D) and Henry's constant (m) for EA as 1.026×10^{-6} m^2 h^{-1} and 0.00235, respectively [28]. The values of biofilm thickness are reported in Table 3. An increasing trend was observed for the biofilm thickness for different phases.

3. Modified Ottengraf Model

In the Ottengraf model, two different equations are proposed: reaction limitation area and diffusion limitation area. The transition between the two conditions is ruled by the Thiele number. This model gives a mathematical continuity to the two Ottengraf equations. In this way, the contribution of both phenomena can be considered simultaneously. We tested the modified model with experimental data obtained in this study and also used the modified Ottengraf model. This new model considers both diffusion and reaction limitations as a single equation.

4. Fundamentals of the New Model

Ottengraf's model individuates two different phenomena, ruling and determining the rate of the biofiltration process. At low load values, diffusion is the rate determining step and, in such conditions, the elimination capacity is given by the following equation:

$$EC_{dL} = L\left(1 - \left(1 - A_s \sqrt{\frac{k_0 D}{2m}} \sqrt{\frac{V}{QL}}\right)^2\right) \tag{23}$$

where the index dl stands for diffusion limiting. Otherwise, at high loads, the removal of the EA is mainly influenced by the biological reaction and the elimination capacity is load-independent.

$$EC_{rl}=EC_{max}=A_s k_0 \delta \quad (24)$$

But, having the use of one equation, only that can continuously connect the different expression of EC_{dl} and EC_{rl} which can be very useful for biofiltration design. The following equation can satisfy this condition:

$$EC = EC_{max} + \frac{(EC_{dl} - EC_{max})}{1+\left(\frac{L}{L^*}\right)^p} \quad (25)$$

where L* is the load at which the transition between reaction and diffusion limitation occurs: for L<L*, conditions of diffusion limiting area are verified, while for L>L* the bioreaction is the rate determining step. For L<<L*, the denominator of the second term on the right side becomes equal to 1 and in such conditions, $EC \equiv EC_{dl}$. Similarly, for L>>L*, all the second term on the right side becomes zero, and therefore $EC \equiv EC_{rl}$. Parameter p was calculated by fitting of the experimental data. Its value specifies the rate at which the passage between the two different limiting conditions occurs. Having a sole equation has many advantages, including the possibility to correlate directly the removal efficiency to the load and to the inlet concentration. Indeed,

$$\eta = \frac{C_i - C_o}{C_i} = \frac{EC}{L} = \left(EC_{max} + \frac{(EC_{dl} - EC_{max})}{1+\left(\frac{L}{L^*}\right)^p} \right) / L \quad (26)$$

With some arithmetical steps and using the definition of L and EC, it is also possible to write efficiency and C_o as a function of C_i:

$$\eta = \frac{\left(A_s k_o \delta + \frac{\frac{C_i Q}{V}\left(1-\left(1-A_s\frac{V}{Q}\sqrt{\frac{k_o D}{2mC_i}}\right)^2\right)}{1+\left(\frac{C_{g,in}}{C_g^*}\right)^p} \right)}{\frac{C_i Q}{V}} \quad (27)$$

$$C_o = C_i - \left[\frac{Q \cdot A_s k_o \delta}{V} + \frac{C_i\left(1-\left(1-A_s\frac{V}{Q}\sqrt{\frac{k_o D}{2mC_i}}\right)^2\right) - A_s k_o \delta}{1+\left(\frac{C_i}{C^*}\right)^p} \right] \quad (28)$$

where C* is the inlet concentration at which load is equal to the L*, at constant flow rate and volume. This simple modification of Ottengraf's model is not merely an algebraically expedient way to give mathematical continuity to Eqs. (27) and (28). Indeed, it is expected that, inside a biofilter, diffusion and reaction limitation conditions simultaneously occur. This may be due to the progressive reduction of pollutant concentration along the reactor, to the presence of some areas with different superficial velocities and to changes in the thickness of the (biomass/solid) film. However, in the new model, as inlet load increases, limitations caused by diffusion reduce and the ones caused by reaction become stronger. The original Ottengraf model and the modified model were compared with the experimental data and are depicted in Figs. 6-9. It was noticed that for this parameters set, the modified model individuates an area with efficiency higher than 100% at very low load values. The arbitrary choice of the parameter p could also cause this anomaly.

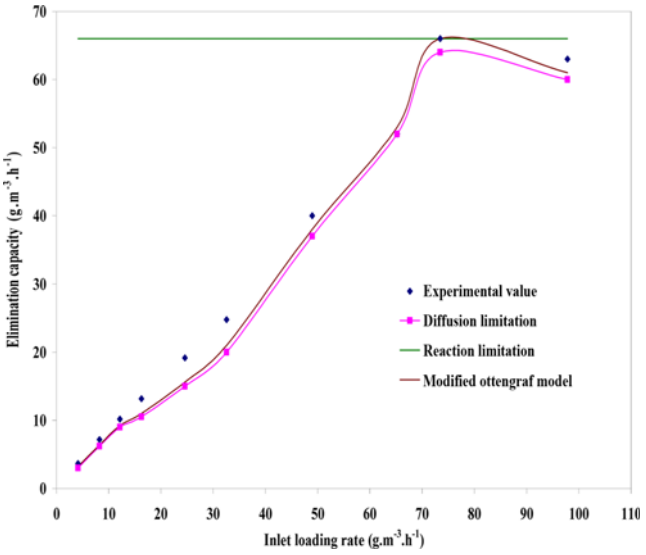

Fig. 6. Comparison of ottengraf model and modified ottengraf model with experimental values for ethylacetate removal in a pressmud based biofilter.

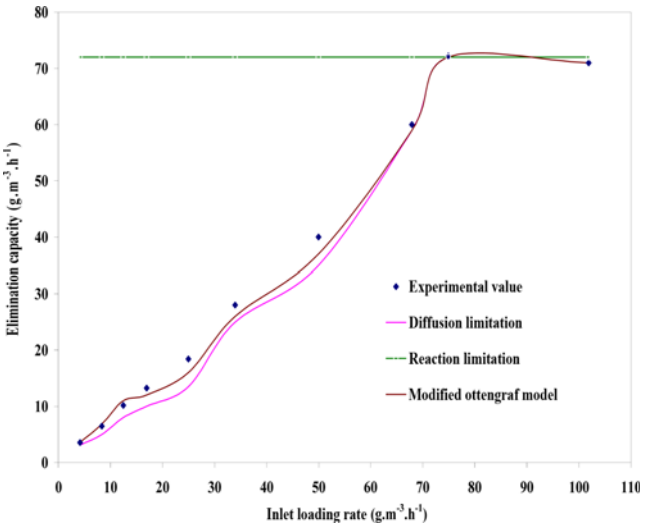

Fig. 7. Comparison of ottengraf model and modified ottengraf model with experimental values for ethylacetate removal in a sugarcane bagasse based biofilter.

5. Modified Ottengraf Model - Advantages and Limitations

Since it is based on Ottengraf studies, the model has the same limitations. First, it is restricted to stationary conditions. The response of the system to external variations is thus not considered. However, it can be used for a first attempt or to evaluate how parameters vary during the operation. In addition, the degradation rate follows a zero-order kinetic. This assumption may be valid for high inlet concentrations and for very soluble pollutants. Indeed, it has been demonstrated that for certain types of contaminants, first-order kinetic prevails [22]. Oxygen limitations are also not considered in the kinetic model. Stratification of the biofilm along the reactor and the contribution of the moisture level are also not included in the model. In addition, the Ottengraf model deals with conventional

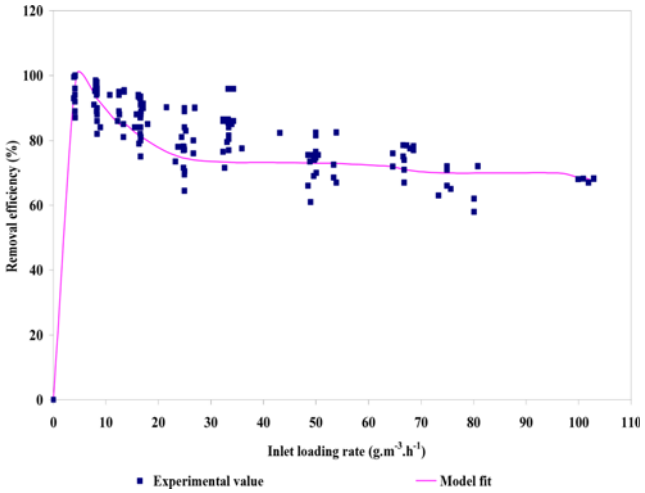

Fig. 8. Comparison of experimental and model predicted values for RE of ethylacetate using pressmud based biofilter.

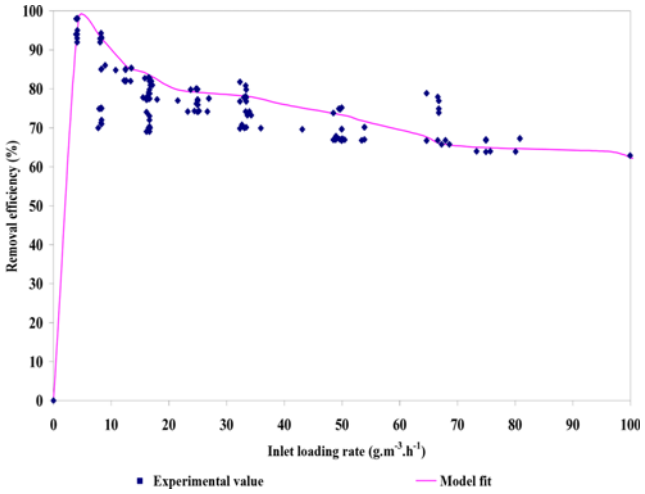

Fig. 9. Comparison of experimental and model predicted values for RE of ethylacetete using sugarcane bagasse based biofilter.

biofilters; hence it does not consider the effects of the biofilter on the removal efficiency. Anyway, the Ottengraf-modified model furnishes one equation for the entire range of mass loading rate and, thereby, many equations can be written to relate loads, concentration, elimination capacity and efficiency.

6. Data Fitting

Experimental data are fitted by using the modified Ottengraf model. This model relates the elimination capacity and the mass loading rate by the following equation:

$$EC = A_s k_o \delta + \left[\frac{L\left(1-\left(1-A_s\sqrt{\frac{k_o D}{2m}}\sqrt{\frac{V}{QL}}\right)^2\right) - A_s k_o \delta}{1+\left(\frac{L}{L^*}\right)^p} \right] \quad (29)$$

and the calculation of the removal efficiency can be easily obtained by using the definitions of EC and L:

$$RE = \frac{C_i - C_o}{C_i} \times 100 = \frac{EC}{L} \times 100 \quad (30)$$

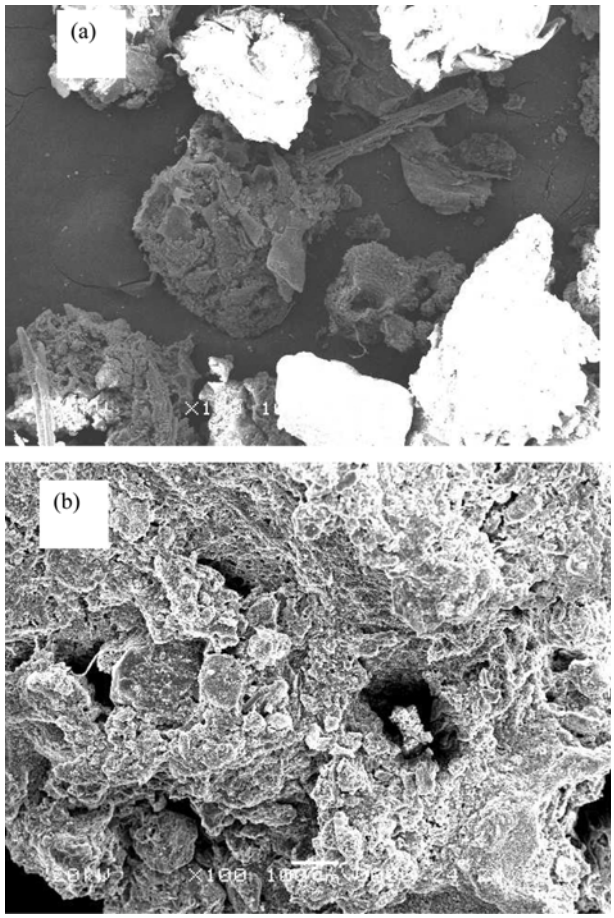

Fig. 10. Biofilm morphology of microorganisms on the surface of pressmud by SEM: (a) at the beginning of biofiltration (b) after 160 days operation (100×).

EC and L data used for data fitting are obtained during the test to assess EC_{max}. Fixed and calculated parameters are reported in Table 3 for BF1 and BF2. The value of L* for the initial set was determined by using the definition of the critical Thiele module as referred by Ottengraf,

$$\phi_{cr} = \delta\sqrt{\frac{k_o m}{DC^*}} = \sqrt{2} \quad (31)$$

Indeed, as previously described, the transition between the reaction and the diffusion limitation area occurs at $\Phi_{cr}=\Phi$ or at $C_i=C^*$.

Using the definition of mass loading rate, L* can be thus expressed as follows:

$$L^* = \frac{C^* Q}{V} = \frac{\delta^2 k_o Q}{2DV} \quad (32)$$

Fitting was carried out for IL vs EC for BF1 and BF2, shown in Figs. 6 and 7, respectively. The final parameter set was successively used to calculate the dependence of the removal efficiency on the inlet loading rate. Figs. 8 and 9 report the model fitting for RE vs inlet loading rate for BF1 and BF2, respectively. There is good agreement between experimental and calculated data. The transition values between diffusion and reaction limitation (critical inlet load) area are given in Table 3. In spite of all the limits encountered and discussed, the new model has a good agreement with the experimen-

tal data.

MICROSCOPIC OBSERVATIONS

The scanning electron micrograph (SEM) can provide information about the microbial community on the biofilter media. The biomass of an individual particle can be mapped. From such precision, important factors such as filter media coverage, thickness and activity can be determined. The SEM of microbial growth on various types of media before and after experiment has already been shown by some researchers [29,30]. A comparison of the scanning electron microscopic images of sugar cane bagasse and pressmud before and after experiment is shown in Figs. 10(a) and 10(b) and Figs. 11(a) and 11(b), respectively. Compared to the initial packing material, a biofilm on the surface of the packing material was observed clearly after 160 days of operation. Even growths of microbial community on the surface of the pore of the packing materials are clearly visible. Initially, the degree of acclimatization was found to be dependent on the adaptive capacity of the microorganism in the packing material, substrate concentration and its availability and on other necessary environmental conditions. Several groups of microorganisms are involved in the degradation of air pollutants in biofilters including bacteria, actinomycetes and fungi [31].

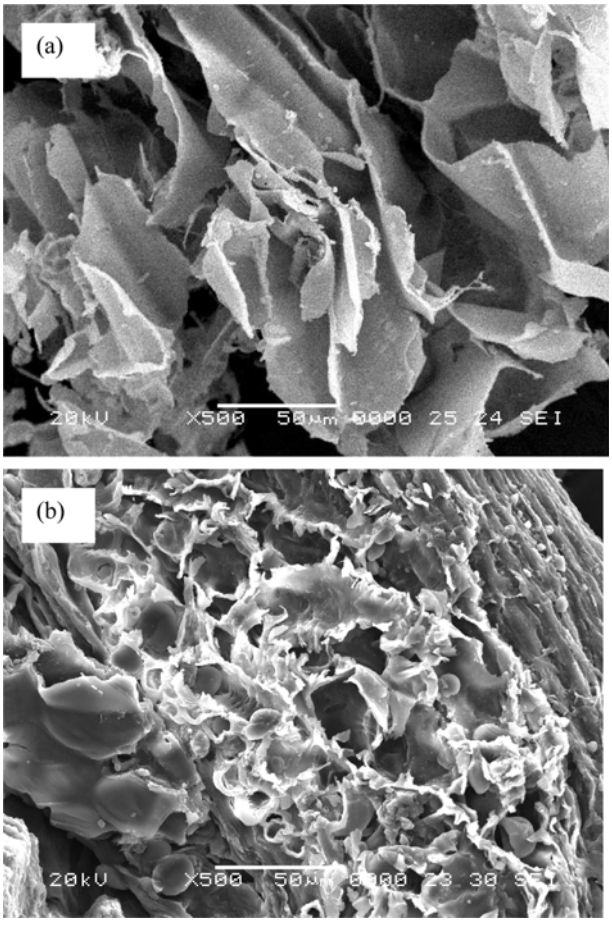

Fig. 11. Biofilm morphology of microorganisms on the surface of sugarcane bagasse by SEM: (a) at the beginning of biofiltration (b) after 160 days operation (500×).

CONCLUSION

The performance of the biofilter was investigated for 160 days. The effect of EA inlet concentrations and gas flow rates on RE and EC was tested. Ottengraf-van den Oever model and modified Ottengraf's model were tested, and fitting demonstrated a good agreement between calculated and experimental data. The modified model has many advantages, including the possibility to have a simple analytical solution. The new model shows good agreement between calculated data and the physics of the process, so it could represent a good mathematical mean for a preliminary process design.

NOMENCLATURE

A_s : specific surface area [m^2m^{-3}]
BF1 : pressmud based biofilter
BF2 : sugarcane bagasse based biofilter
C* : pollutant concentration in the gas flow at which passage between reaction and diffusion limitation area occurs [gm^{-3}]
C_{go} : outlet pollutant concentration [gm^{-3}]
$C_{o,\,Critical}$: critical concentration [gm^{-3}]
C_g : pollutant concentration [gm^{-3}]
C_i : inlet pollutant concentration [gm^{-3}]
D : diffusion coefficient [m^2h^{-1}]
EC_{dl} : elimination capacity referred to reaction limitation area [$gm^{-3}h^{-1}$]
EC_{max} : maximum elimination capacity [$gm^{-3}h^{-1}$]
EC_{rl} : elimination capacity referred to diffusion limitation area [$gm^{-3}h^{-1}$]
H : distance from the bed [m]
k_1 : first-order kinetic constant [h^{-1}]
K_g : microbial growth rate
K_m : saturation (Michaelis-Menten) constant (gm^{-3}) in the gas phase
k_o : zero-order kinetic constant [$gm^{-3}h^{-1}$]
L* : load at which the transition between reaction and diffusion limitation [gm^{-3}]
L_c : critical mass loading rate [$gm^{-3}h^{-1}$]
N : flux of substrate from the gas to the solid [$gm^{-2}h^{-1}$]
P : parameter of the Ottengraf-modified model
PCO_2 : carbon dioxide production rate [$gm^{-3}h^{-1}$]
Q : volumetric flow rate [m^3s^{-1}]
R : overall reaction rate [$gm^{-3}h^{-1}$]
r_{max} : maximum biodegradation rate per unit biofilter volume [$gm^{-3}h^{-1}$]
T : operation time [h]
V : volume of the reactor [m^3]
U_g : superficial velocity [m s^{-1}]
X : number of viable cells per unit volume

REFERENCES

1. D. Wu, X. Quan, Y. Zhao and S. Chen, *J. Hazard. Mater.*, **136**, 288 (2006).
2. C. Kennes and M. C. Veiga, *J. Biotechnol.*, **113**, 305 (2004).
3. J. W. Van Groenestijn and P. G. M. Hesselink, *Biodegradation*, **4**, 283 (1993).

4. J. S. Devinny and D. S. Hodge, *J. Air Waste Manage. Assoc*., **45**, 125 (1995).
5. A. J. Daugulis and N. G. Boudreau, *Biotechnol. Lett.*, **25**, 1421 (2003).
6. E. Ramírez-López, J. Corona-Hernández, L. Dendooven, P. Rangel and F. Thalasso, *Bioresour. Technol*., **88**, 259 (2003).
7. H. L. Bohn, *Chem. Eng. Prog*., **88**, 34 (1992).
8. A. Pandey, C. R. Soccol, P. Nigam and V. T. Soccol, *Bioresour. Technol*., **74**, 69 (2000).
9. M. Zilli, D. Daffonchio, R. Di. Felice1, M. Giordani and A. Converti, *Biodegradation*, **15**, 87 (2004).
10. W. C. Chan and R. X. Zheng, *J. Chem. Technol. Biotechnol.*, **80**, 574 (2005).
11. L. Bibeau, K. Kiared, A. Leroux, R. Brzezinski, G. Viel and M. Heitz, *Can. J. Chem. Eng.*, **75**, 921 (1997).
12. H. M. Tang and S. J. Hwang, *J. Air Waste Manage. Assoc.*, **47**, 1142 (1997).
13. C. W. Lin and Y. W. Cheng, *J. Chem. Technol. Biot.*, **82**, 51 (2007).
14. H. Jorio, R. Brzezinski and M. Heitz, *J. Chem. Technol. Biot.*, **80**, 796 (2005).
15. J. P. Arcangeli and E. Arvin, *Biodegradation*, **10**, 177 (1999).
16. M. E. Acuna, F. Perez, R. Auria and S. Revah, *Biotechnol. Bioeng.*, **63**, 175 (1999).
17. M. Schirmer, B. J. Butler, J. W. Roy, E. O. Frind and J. F. Barker, *J. Contam. Hydrol.*, **37**, 69 (1999).
18. P. Juteau, R. Laroque, D, Rho and A. Le Duy, *Appl. Microbiol. Biotechnol.*, **52**, 863 (1999).
19. L. H. Smith and P. L. McCarty, *Biotechnol. Bioeng.*, **55**, 650 (1997).
20. H. M. Tang and S. J. Hwang, *J. Air Waste Manage. Assoc*., **47**, 1142 (1997).
21. R. Govind, Z. Wang and D. F. Bishop, *Air and Waste Management Association, Proceedings of the 90th Annual Meeting and Exhibition*, Toronto, Canada (1997).
22. S. P. P. Ottengraf and A. H. C. Vander Oever, *Biotechnol. Bioeng.*, **25**, 3089 (1983).
23. J. S. Devinny and D. S. Hodge, *J. Environ. Eng.*, **121**, 21 (1995).
24. Y. Jin, L. Guo, M. C. Veiga and C. Kennes, *Biotechnol. Bioeng.*, **96**, 433 (2007).
25. M. C. Delhomenie, L. Bibeau and M. Heitz, *Chem. Eng. Sci.*, **57**, 4999 (2002).
26. A. Windsperger, *Radex Rundsch*, **3**, 7 (1991).
27. F. Javier Alvarez-Hornos, V. Carmen Gabaldon, Martínez-Soria, Paula Marzal and Josep-Manuel Penya-roja, *Biochem. Eng. J.*, **43**, 169 (2009).
28. M. Deshusses and C. T. Johnson, *J. Air Waste Marage. Assoc.*, **49**, 973 (1999).
29. W. Namkoonga, J. S. Parka and J. S. Vander Gheynst, *Environ. Poll*, **121**, 181 (2004).
30. K. Chmiel. *Transient and steady state characteristics of butanol biodegradation on a pre-selected pine bark bed,* Ph.D. Thesis, Silesian University of Technology, Gliwice, Poland (2003).
31. G. Leson and A. M. Winer, *J. Air Waste Marage.*, **41**, 1045 (1991).